

## **Title: A hybrid method for generation of attenuation map for MR-based attenuation correction of PET data in prostate PET/MR imaging**

**Authors:** Mehdi Shirin Shandiz<sup>a</sup>, Mohammad Hadi Arabi<sup>a</sup>, Pardis Ghafarian<sup>b</sup>, Mehrdad Bakhshayesh Karam<sup>b</sup>, Hamidreza Saligheh Rad<sup>a</sup> and Mohammad Reza Ay<sup>a</sup>

**Affiliations:** <sup>a</sup>Department of Medical Physics and Biomedical Engineering and Research Center for Molecular and Cellular Imaging, Tehran University of Medical Sciences, Tehran, Iran, <sup>b</sup>Chronic Respiratory Disease Research Center, NRITLD and PET/CT and Cyclotron Center, Masih Daneshvari Hospital, Shahid Beheshti University of Medical Sciences, Tehran, Iran

### **Aim:**

Recently introduced PET/MRI scanners present significant advantages in comparison with PET/CT including better soft-tissue contrast, lower radiation dose, and truly simultaneous imaging capabilities. However, the lack of accurate method for generation of attenuation map ( $\mu$ map) at 511 keV from MR images for implementation of MR-based attenuation correction (MRAC) is hampering further development and wider acceptance of this technology. This issue is more pronounced during the imaging area with large bony structures such as pelvis in prostate imaging. In this study, we present a new method including short echo-time (STE) pulse sequence to detect bone signal along with a robust and automatic image segmentation method base on FCM, active contouring and shape analysis to provide a three class attenuation map including bone, air and soft tissue in pelvis region.

### **Methods and materials:**

The proposed imaging protocol implemented on a clinical 1.5T Avanto (Siemens Medical Solution, Erlangen, Germany) scanner. The acquisition parameters were 1.11 msec and 20 msec for TE and TR, respectively, with FA=20. The image-processing protocol includes five major steps, illustrated in figure 1, and as follows: (I) intensity-inhomogeneity correction using non parametric method, which is an essential step for removing bias field, mainly produced by imperfections in the radiofrequency coils and object dependent interactions; (II) separation of bone and air from other areas using active contouring based on gradient vector method; (III) FCM in order to segment the image into two clusters, one cluster is bone and air and another cluster is soft tissue; (IV) separation of bone and air areas using shape analysis; and (V) generation of  $\mu$ map. The accuracy of the proposed segmentation method was validated using comparison against manual segmentation performed by an expert radiologist.

### **Results:**



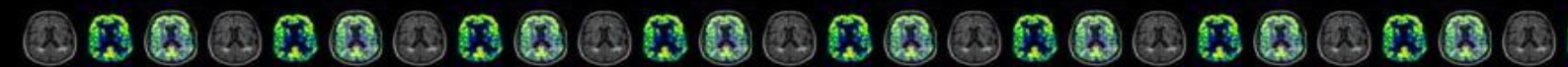
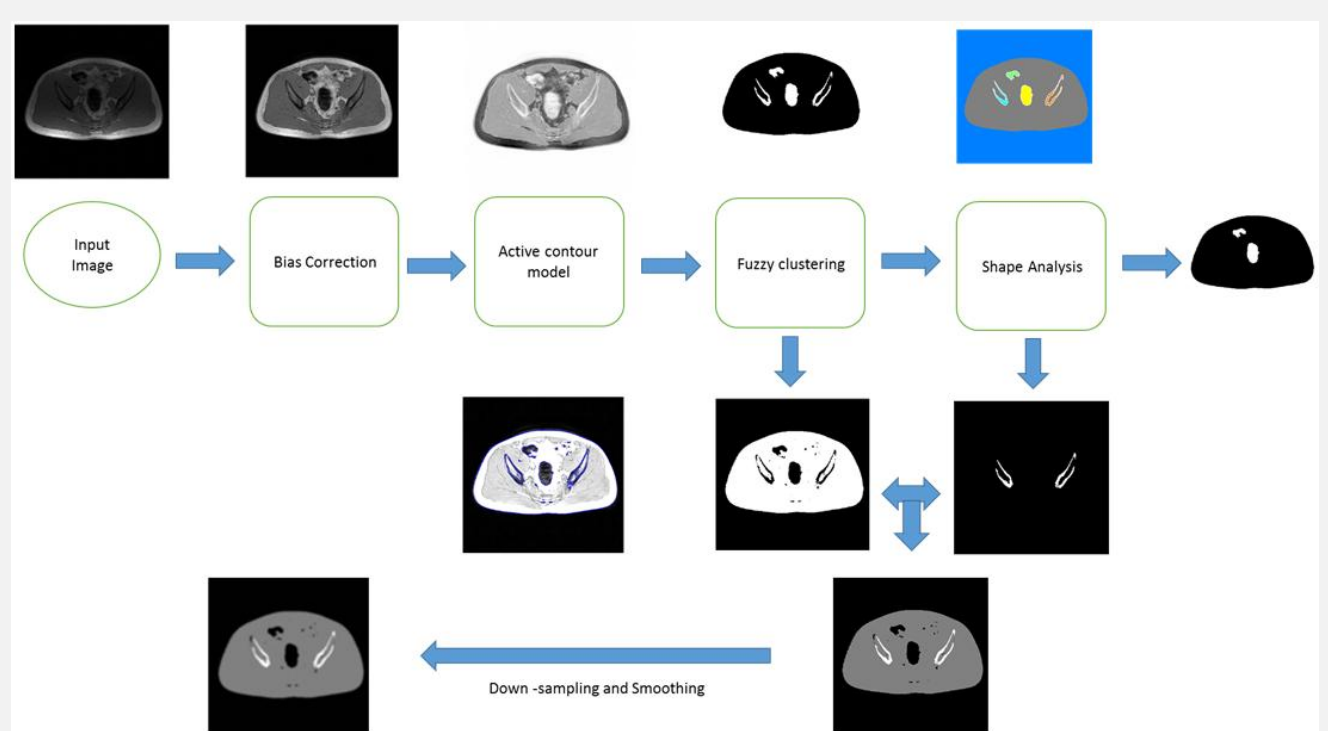


Figure 2 shows two slices acquired from pelvic area of a male volunteer by STE pulse sequence following by image processing steps, the corresponding segmentation images and generated attenuation  $\mu$ map in 511 keV prove the validity of algorithm. Table 1 shows quantitate analysis on accuracy, sensitivity and specificity for 15 segmented images in comparison with manual segmentation performed by an expert radiologist.

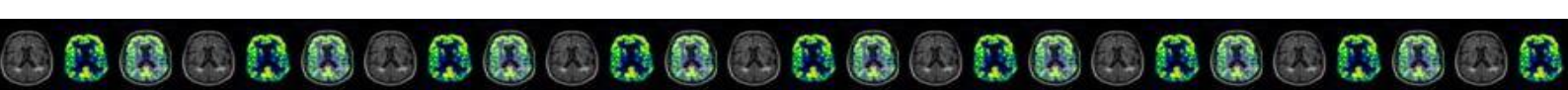
**Discussion – Conclusion:**

The proposed strategy in this study shows that the three tissue class  $\mu$ map can be successfully generated from MR images in pelvis region using STE pulse sequence following by the image processing steps. The proposed method can be a potential alternative to UTE-based PET attenuation correction, particularly in more common hybrid PET/MRI systems. The proposed method needs to be examined in bigger patient population. The algorithm is still under development and will be validated in more details based on comparison with the  $\mu$ maps generate from CT images. This study has been developed particularly for improving the accuracy of MRAC in prostate imaging which is one of the killer applications of hybrid PET/MR imaging.

**Supplementary Figures and Tables:**



**Figure 1.** The workflow of the proposed algorithm for generation of  $\mu$ map at 511 keV from MR image acquired using a single STE pulse sequence



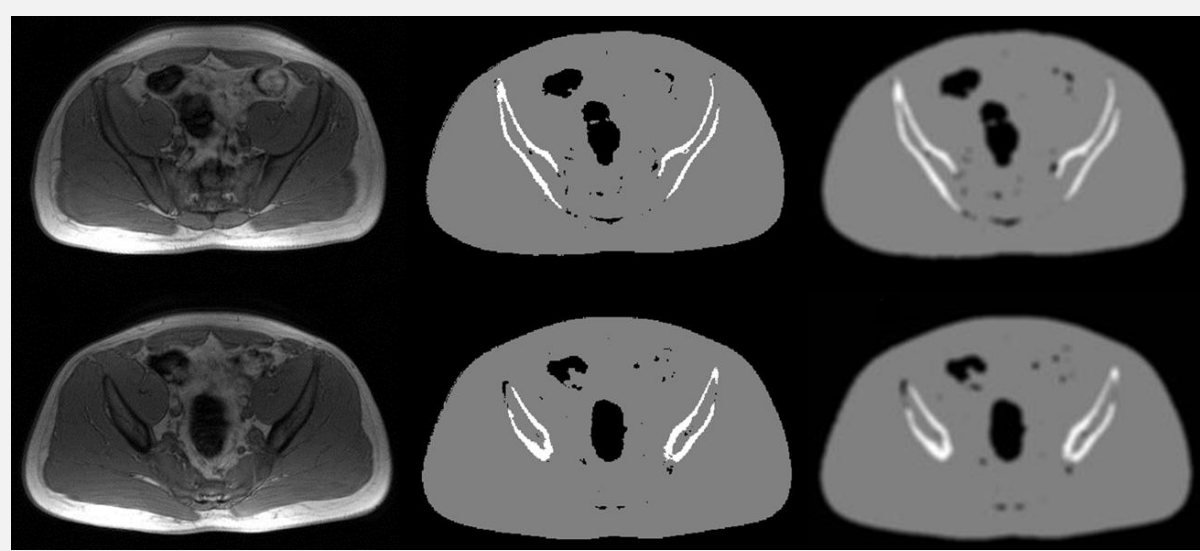
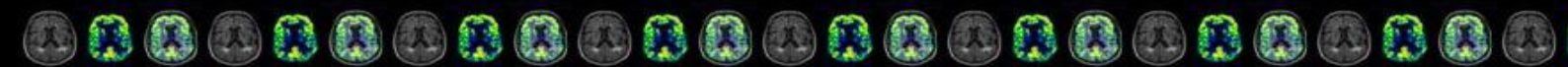


Figure 2. MR image acquired using STE pulse sequence (left); three class segmented image (middle); generated  $\mu$ map (right)

Table 1. Evaluation of proposed method with comparison with manual segmentation implemented by an expert radiologist

	Accuracy (mean $\pm$ SD)	Sensitivity (mean $\pm$ SD)	Specificity (mean $\pm$ SD)
Bone	0.993 $\pm$ 0.0062	0.998 $\pm$ 0.0023	0.63 $\pm$ 0.2173
Air	0.995 $\pm$ 0.0045	0.997 $\pm$ 0.0029	0.60 $\pm$ 0.1330

